Check for updates

Methane budget estimates in Finland from the CarbonTracker Europe-CH$_4$ data assimilation system

By AKI TSURUTA[1]*, TUULA AALTO[1], LEIF BACKMAN[1], MAARTEN C. KROL[2,3,4], WOUTER PETERS[2,5], SEBASTIAN LIENERT[6], FORTUNAT JOOS[6], PAUL A. MILLER[7], WENXIN ZHANG[8], TUOMAS LAURILA[1], JUHA HATAKKA[1], ARI LESKINEN[1,9], KARI E. J. LEHTINEN[1,9], OLLI PELTOLA[1], TIMO VESALA[10,11], JANNE LEVULA[10], ED DLUGOKENCKY[12], MARTIN HEIMANN[10,13], ELENA KOZLOVA[14], MIKA AURELA[1], ANNALEA LOHILA[1], MARI KAUHANIEMI[1], and ANGEL J. GOMEZ-PELAEZ[15†]

[1]*Finnish Meteorological Institute, Helsinki, Finland;* [2]*Meteorology and Air Quality, Wageningen University & Research, Wageningen, The Netherlands;* [3]*SRON Netherlands Institute for Space Research, Utrecht, The Netherlands;* [4]*Institute for Marine and Atmospheric Research Utrecht, Utrecht University, Utrecht, The Netherlands;* [5]*Centre for Isotope Research, Energy and Sustainability, Research Institute Groningen, Groningen University, Groningen, The Netherlands;* [6]*Climate and Environmental Physics, Physics Institute & Oeschger Centre for Climate Change Research, University of Bern, Bern, Switzerland;* [7]*Department of Physical Geography and Ecosystem Science, Lund University, Lund, Sweden;* [8]*Department of Geosciences and Natural Resource Management, Center for Permafrost (CENPERM), University of Copenhagen, Copenhagen, Denmark;* [9]*Department of Applied Physics, University of Eastern Finland, Kuopio, Finland;* [10]*University of Helsinki, Faculty of Science, Institute for Atmospheric and Earth System Research (INAR)/Physics, University of Helsinki, Finland;* [11]*University of Helsinki, Faculty of Science, Institute for Atmospheric and Earth System Research (INAR)/Forest Sciences, University of Helsinki, Finland;* [12]*Global Monitoring Division, NOAA Earth System Research Laboratory, Boulder, CO, USA;* [13]*Max Planck Institute for Biogeochemistry, Jena, Germany;* [14]*College of Life and Environmental Sciences, University of Exeter, Exeter, UK;* [15]*Meteorological State Agency of Spain (AEMET), Tenerife, Spain*

ABSTRACT

We estimated the CH$_4$ budget in Finland for 2004–2014 using the CTE-CH$_4$ data assimilation system with an extended atmospheric CH$_4$ observation network of seven sites from Finland to surrounding regions (Hyytiälä, Kjølnes, Kumpula, Pallas, Puijo, Sodankylä, and Utö). The estimated average annual total emission for Finland is 0.6 ± 0.5 Tg CH$_4$ yr^{-1}. Sensitivity experiments show that the posterior biospheric emission estimates for Finland are between 0.3 and 0.9 Tg CH$_4$ yr^{-1}, which lies between the LPX-Bern-DYPTOP (0.2 Tg CH$_4$ yr^{-1}) and LPJG-WHyMe (2.2 Tg CH$_4$ yr^{-1}) process-based model estimates. For anthropogenic emissions, we found that the EDGAR v4.2 FT2010 inventory (0.4 Tg CH$_4$ yr^{-1}) is likely to overestimate emissions in southernmost Finland, but the extent of overestimation and possible relocation of emissions are difficult to derive from the current observation network. The posterior emission estimates were especially reliant on prior information in central Finland. However, based on analysis of posterior atmospheric CH$_4$, we found that the anthropogenic emission distribution based on a national inventory is more reliable than the one based on EDGAR v4.2 FT2010. The contribution of total emissions in Finland to global total emissions is only about 0.13%, and the derived total emissions in Finland showed no trend during 2004–2014. The model using optimized emissions was able to reproduce observed atmospheric CH$_4$ at the sites in Finland and surrounding regions fairly well (correlation > 0.75, bias $< \pm 7$ ppb), supporting adequacy of the observations to be used in atmospheric inversion studies. In addition to global budget

*Corresponding author. e-mail: aki.tsuruta@helsinki.fi
[†]At present: AEMET, Delegation in Asturias, Izaña Atmospheric Research Center, Oviedo, Spain

1

estimates, we found that CTE-CH$_4$ is also applicable for regional budget estimates, where small scale ($1^\circ \times 1^\circ$ in this case) optimization is possible with a dense observation network.

1. Introduction

Methane (CH$_4$) is the second most important anthropogenic greenhouse gas after carbon dioxide (CO$_2$). The atmospheric abundance of CH$_4$ is directly influenced by anthropogenic emissions and the increase in CH$_4$ mole fraction since pre-industrial time induced an effective radiative forcing of $+0.50 \pm 0.05$ W m^{-2} (update of Hofmann et al. (2006), https://www.esrl.noaa.gov/gmd/aggi/aggi.html). CH$_4$ is emitted from both anthropogenic and natural sources. Major sources of anthropogenic CH$_4$ emissions include emissions from solid fuels, gas and oil production and distribution, agriculture (e.g. enteric fermentation and rice fields), waste management (landfills) and biomass burning, which in total accounts for more than half of global emissions (Kirschke et al., 2013; Saunois et al., 2016). Major sources of natural CH$_4$ emission are wetlands and peatlands, accounting for about 30% of global emissions (Kirschke et al., 2013; Saunois et al., 2016).

Boreal and subarctic terrestrial land is covered by a large areas of peatlands, where about one fifth of global terrestrial carbon is stored (Ciais et al., 2013). The processes related to CH$_4$ fluxes from northern boreal regions have been extensively studied (e.g. Christensen et al., 1996; Nykänen et al., 1998; Rinne et al., 2007; Aurela et al., 2009; Lohila et al., 2011; Emmerton et al., 2016; Dinsmore et al., 2017), and show that CH$_4$ fluxes are highly sensitive to climatic drivers that vary seasonally and inter-annually (Christensen et al., 2003). In addition, CH$_4$ fluxes from wetlands and peatlands are highly heterogeneous in space (Frolking and Crill, 1994; Moore et al., 1994). Even between points separated by distances of a few meters or less, CH$_4$ fluxes can differ by orders of magnitude (Moore et al., 1998). Therefore, upscaling and modelling of CH$_4$ fluxes on regional scales has been challenging, and the estimates still have large uncertainties (Petrescu et al., 2010; Wania et al., 2013; Cresto Aleina et al., 2016; Fisher et al., 2017).

Natural emissions in Finland, where substantial areas of pristine peatlands are located, are an important part of the regional methane budget (Minkkinen et al., 2002; Huttunen et al., 2003; Monni and Benviroc Ltd, 2013; Statistics Finland, 2015). Anthropogenic emissions from Finland are relatively small compared to, e.g. Asia, America, Russia and central Europe, due to the limited number of large cities and lower emissions from agricultural activities. However, their magnitude is comparable to that of natural emissions, contributing about equally to the country and regional budgets.

Anthropogenic CH$_4$ emissions from Fennoscandia are assumed to have a small seasonal variation and large uncertainty in their spatial distribution. Emission inventories, such as that by the Emission Database for Global Atmospheric Research (EDGAR; see http://edgar.jrc.ec.europa.eu/terms_of_use.php) and ECLIPSE (Stohl et al., 2015) provide gridded global anthropogenic emission estimates that have been used for global and regional studies (e.g. Bergamaschi et al., 2005, 2018; Houweling et al., 2014, 1999; Thompson et al., 2017). Although the EDGAR inventory has the advantage of providing a continuously updated emission distribution on a small scale ($0.1^\circ \times 0.1^\circ$), possible biases between the Northern and Southern Hemispheres and between countries, have been discussed in previous studies (Houweling et al., 2014; Bergamaschi et al., 2015).

In this study, we examine CH$_4$ emission estimates in Finland for 2004–2014 using the CarbonTracker Europe-CH$_4$ (CTE-CH$_4$) data assimilation system (Tsuruta et al., 2017), with an extended observation network in Finland and surrounding regions. Previously, observations from only one site in Finland (Pallas, Finland) have been used for inversion studies (Bergamaschi et al., 2005, 2015, 2018; Bousquet et al., 2011; Monteil et al., 2013; Bruhwiler et al., 2014; Houweling et al., 2014; Thompson et al., 2017), but we improve the analysis in this study by including seven sites. Sensitivity of inversion estimates to the observations is examined by using two different sets of the newly assimilated observations. In addition, we examine the seasonal cycles and the spatial distributions of prior emissions by using three different biospheric and two different anthropogenic prior emission estimates. The biospheric priors are from LPJ-GUESS (Wetland Hydrology and Methane version) (henceforth LPJG-WHyMe) (Smith et al., 2001; Wania et al., 2009; McGuire et al., 2012), LPX-Bern version 1.0 (v1.0) with prescribed peat- and wetland extent (Spahni et al., 2013) and LPX-Bern (v1.0) including the DYPTOP (Dynamical Peatland Model Based on TOPMODEL) module to simulate peat- and wetland extent (Stocker et al., 2014). The two priors for anthropogenic emissions are from
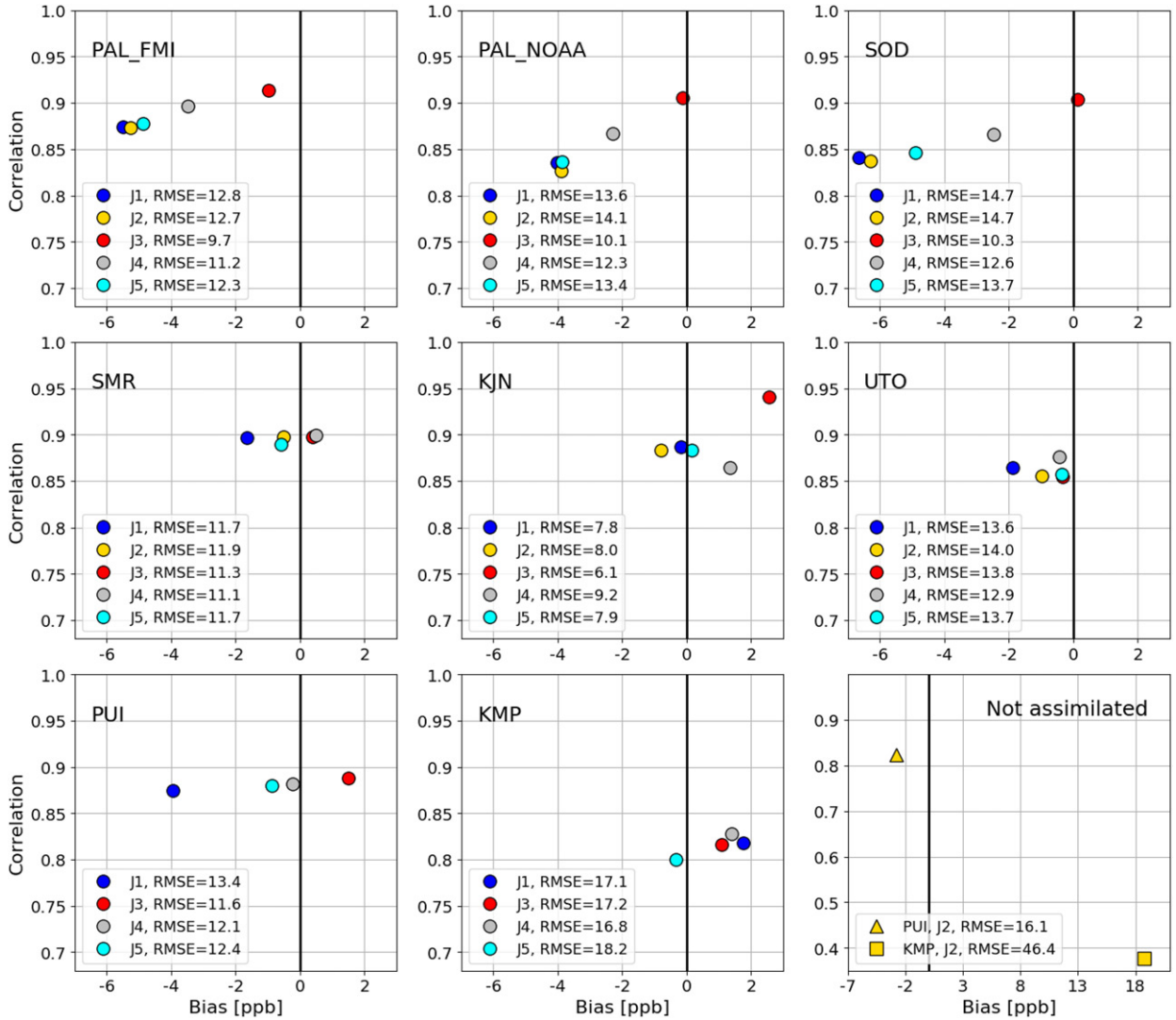
Fig. 1. Statistics (bias, correlation and root mean squared error (RMSE)) of posterior atmospheric CH_4 compared with assimilated observations from sites in Finland and surrounding regions. Negative bias shows model underestimation. The statistics were calculated from 2010–2014 observations, except for KJN, where 2013–2014 data were used. The statistics for Puijo (PUI) and Kumpula (KMP) for J2 were plotted separately, as those were not assimilated in J2, and the statistics are calculated from posterior estimates and all prepossessed daily observations.

EDGAR v4.2 FT2010 and a combination of EDGAR and the Finnish national inventory.

2. Methods and datasets

2.1. CTE-CH₄

CTE-CH₄ is a branch of the CarbonTracker Europe data assimilation system (Peters et al., 2005; van der Laan-Luijkx et al., 2017) that optimizes global CH_4 fluxes (Tsuruta et al., 2017). The system is based on an ensemble Kalman smoother with a fixed lag assimilation window (Ravela and McLaughlin, 2007), with 500 ensemble members and an assimilation window of 5 weeks. We used the TM5 atmospheric chemistry transport model (Krol et al., 2005) as an observation operator.

TM5 is driven by ECMWF ERA-Interm meteorological fields, and runs on a $1° \times 1°$ zoom grid over Europe (up to 74°N), $6° \times 4°$ globally with an intermediate $3° \times 2°$ zoom region (Supporting Information Fig. 3). Vertical mixing in TM5 was calculated based on the Gregory et al. (2000) convection scheme as stored in the ERA-Interim meteorological fields. The monthly atmospheric CH_4 sink due to photochemical reactions with OH, Cl, and $O(^1D)$ were taken into account, based on Houweling et al. (2014) and Brühl and Crutzen (1993).
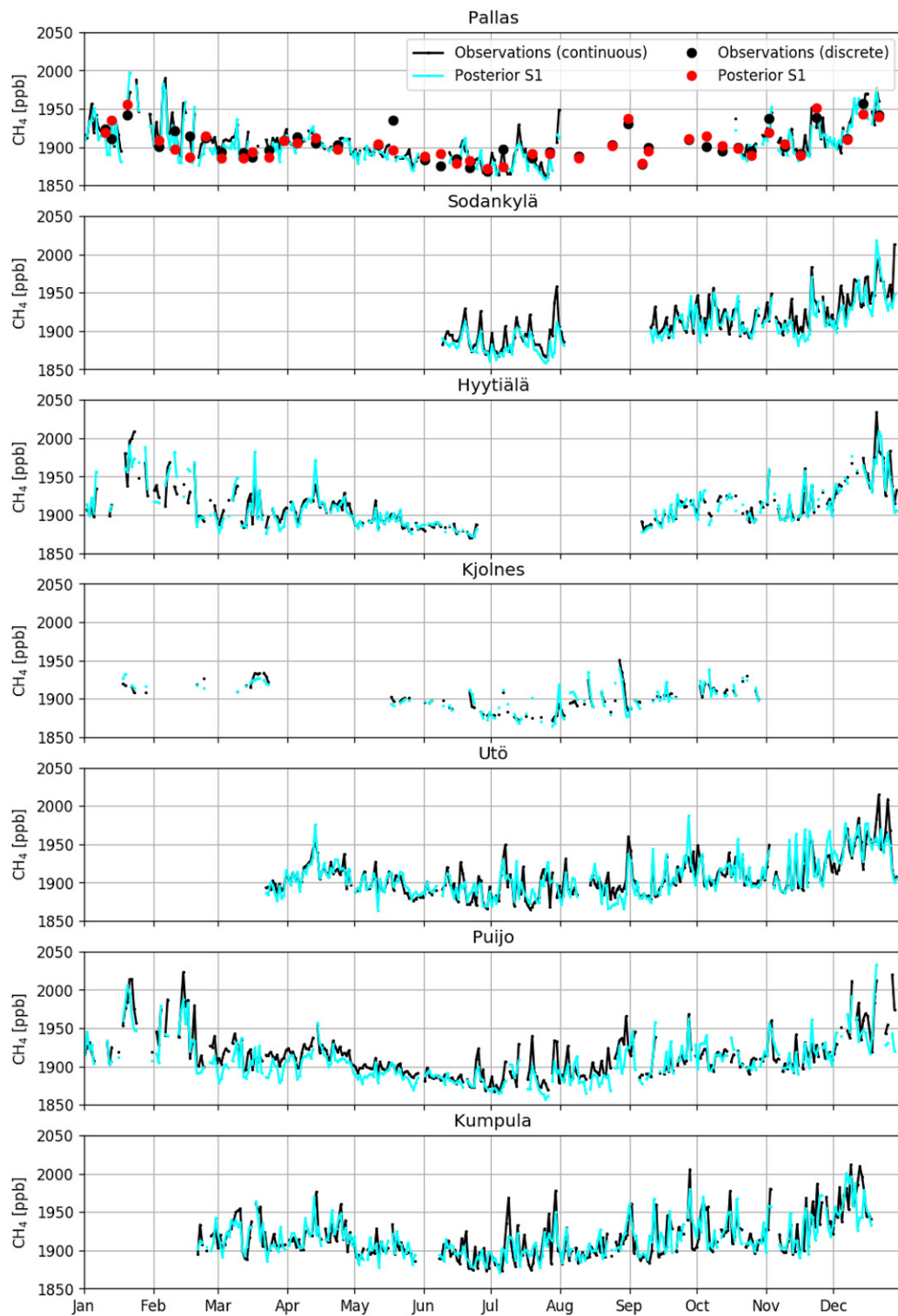
Fig. 2. Observed and simulated atmospheric CH$_4$ at sites in Finland and surrounding regions for 2012, except for Kjølnes which shows data from 2014. For continuous observations, the daily averaged values are shown. For complete time series for all inversions, see Supplementary Material.
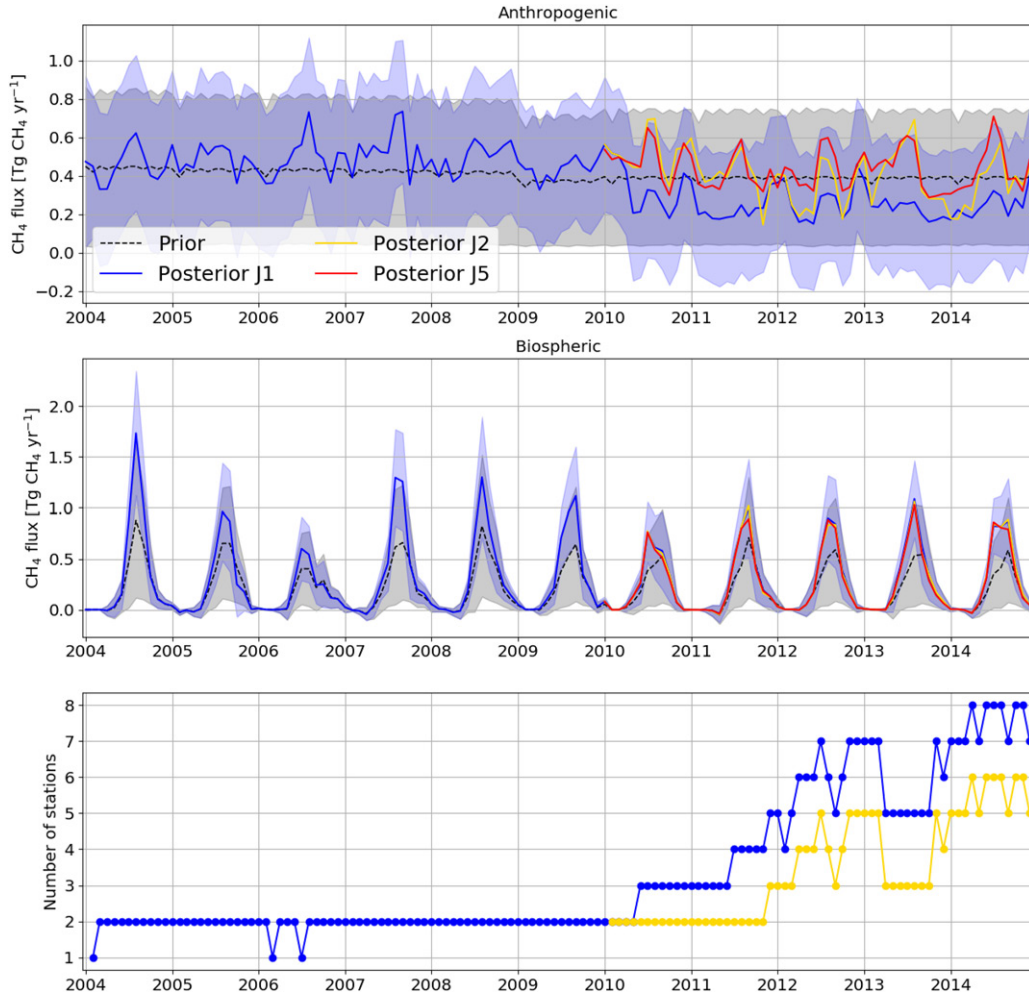
Fig. 3. [Top and middle] Monthly prior and posterior anthropogenic and biospheric emission estimates for Finland. The shaded areas show uncertainty ranges of the prior (grey) and the J1 posterior (blue). [Bottom] Number of Fennoscandian stations assimilated in J1 and J5. Note the number in J2 was same as in J1.

Inter-annual variability of the atmospheric sink was not taken into account, and the atmospheric sink was not adjusted in the optimization scheme.

The fluxes were optimized weekly for 2004–2014 on $1° \times 1°$ resolution over Europe and region-wise elsewhere globally, in order to take advantage of the high observation density in Europe. Results on the $1° \times 1°$ grid are briefly compared to the region-wise approach in Section 4.3. The definition of geographical regions is based on modified TransCom (mTC) regions and a land ecosystem type (LET) map derived from the Dynamical Peatland Model Based on TOPMODEL (DYPTOP; Stocker et al., 2014) (see Supporting Information for details). In this study, both anthropogenic and biospheric fluxes were optimized simultaneously per grid cell over Europe (mTC24-29), yielding individual estimates for anthropogenic and biospheric emissions for each grid cell.

Globally, either anthropogenic or biospheric emissions were optimized, depending on which emission type was dominant (see Tsuruta et al., 2017). This was done per region, but not per grid cell. Although CTE-CH$_4$ is a global model, this study focuses on the estimates in Finland where most of the newly assimilated observations (see Section 2.3) are located. The emission estimates for Finland were calculated from global estimates using a country mask (Supporting Information Fig. 4).

Uncertainty for prior flux estimates are assumed to be 80% of the fluxes over land and 20% over ocean (see Tsuruta et al., 2017). Smaller percentage for ocean was chosen as the emission is smaller relative to land, and we expected difficulties distinguishing the source signal from ocean in the inversion. The prior biospheric fluxes over land were assumed to be correlated between modified TransCom regions with the same LET, with a
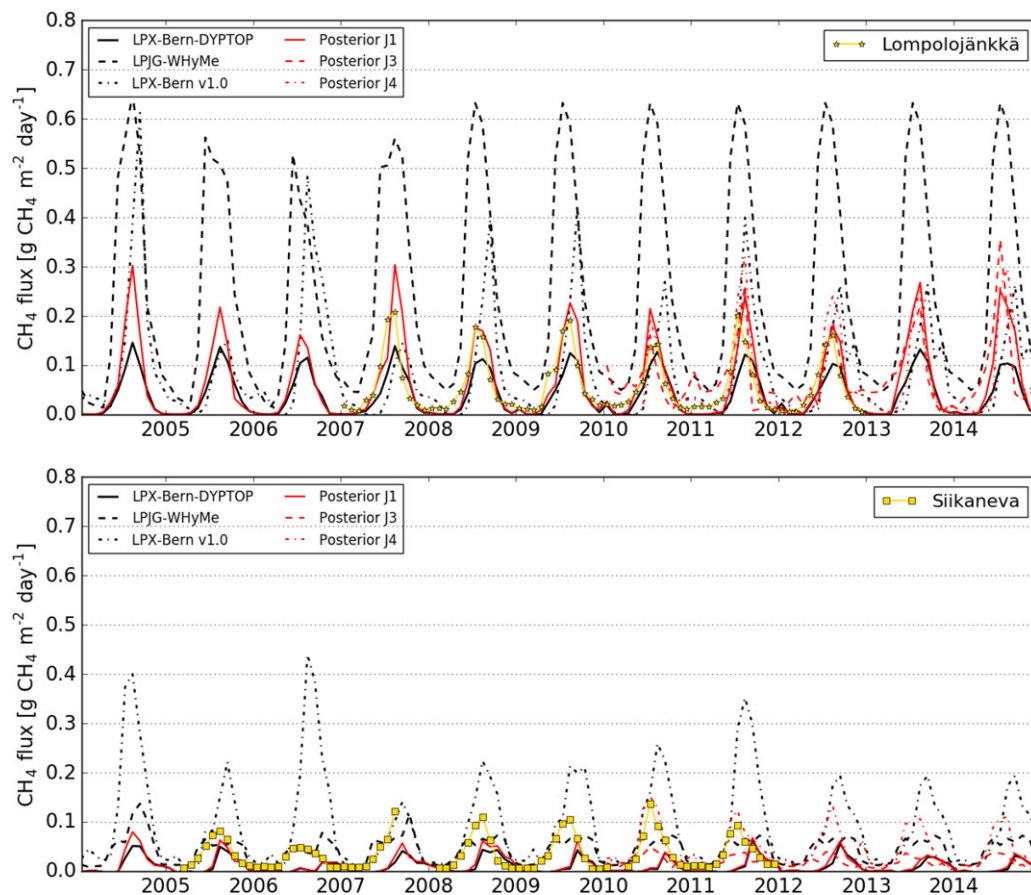
Fig. 4.   Measured CH₄ fluxes at Lompolojänkkä and Siikaneva, and estimated regional monthly mean biospheric CH₄ fluxes around the sites.

correlation length of 500 km, and the anthropogenic fluxes over ocean (mainly consisting of coastal and ship track emissions) were assumed to be correlated between modified TransCom regions with a correlation length of 900 km (see Supporting Information for details). The anthropogenic fluxes were assumed to be uncorrelated over land because there are still uncertainties in the spatial distribution and the timing of, e.g. agricultural emissions in the inventory, which could be improved by the optimization. This assumption is the simplest alternative to a proper error covariance that could be constructed from, e.g. uncertainties in the parameters in the bottom-up inventory. In Europe, the prior biospheric fluxes were assumed to be correlated between grid cells within Europe with a correlation length of 500 km. In this way, the influence of observations is less restricted by the LET in Europe, which allows a higher degree of freedom in the optimization. To better separate the sources, prior anthropogenic and biospheric emissions (see Section 2.2) were assumed to be uncorrelated both in Europe and globally.

2.2. Prior flux estimates

Prior flux estimates have five source categories: anthropogenic, biospheric, fire, termites and ocean. Among those, anthropogenic and biospheric emissions are dominant sources for Finland, contributing to more than 95% of total emissions. Although fluxes from fire, termites and ocean are minor sources of CH₄ for Finland, they were included in the model as their contributions to the global budget and regional budgets elsewhere are significant and needed to close the global budget.

For annual prior anthropogenic emissions, estimates from the EDGAR v4.2 FT2010 inventory were used. The inventory covers data up to 2010, and we assumed 2011–2014 emissions to be same as 2010. Globally, anthropogenic emissions are likely to have increased continuously during 2011–2014 (Schaefer et al., 2016; Schwietzke et al., 2016), but possibly not for Finland. We assumed that the inversion would be able to capture the global increase, as previously shown in Tsuruta et al. (2017). In addition to the EDGAR inventory, we used a modified EDGAR inventory (FIN-EDGAR), where the anthropogenic emission distribution over Finland was

taken from a national inventory (Statistics Finland, 2015; Statistics Finland PX-Web regional database, n.d.). The spatial distribution of the EDGAR inventory for Finland is mainly based on population distribution (e.g. for waste management; EDGAR, 2010), and non-dairy cattle distribution (e.g. for agricultural emissions) by Lerner et al. (1988) (IEA report part III; Olivier and Janssens-Maenhout, 2012). This distribution differs considerably from the national inventory which uses more up-to-date information, and municipality statistics, collected every year from each municipality. Based on the agricultural animal distribution from the national inventory, the sum of emissions from enteric fermentation and manure management in the EDGAR inventory was redistributed. Similarly, based on the landfill distribution, the sum of emissions from solid waste disposal and waste water was redistributed. In FIN-EDGAR, emissions from Finland were scaled to preserve the total emissions from the EDGAR inventory, making the estimates consistent with nearby regions. Anthropogenic emission estimates over the ocean (mainly from coastal and ship track emissions) are taken from the EDGAR inventory, and optimized. Other gridded global anthropogenic estimates are available from, e.g. the EU 7th Framework Programme project ECLIPSE, which provides gridded emission patterns based on the Global Energy Assessment (GEA, 2012). However, the distribution of ECLIPSE emissions over Finland was similar to EDGAR, so we did not use the estimates from ECLIPSE in this study.

For monthly prior biospheric fluxes, estimates from the LPX-Bern-DYPTOP ecosystem model with dynamically simulated peat- and wetland extent (Stocker et al., 2014) were used. In addition, estimates from LPJ-GUESS (Wetland Hydrology and Methane version) (LPJG-WHyMe) (Smith et al., 2001; Wania et al., 2009; McGuire et al., 2012) and LPX-Bern v1.0 with prescribed peat- and wetland area (Spahni et al., 2013) were used for sensitivity analysis. The biospheric flux estimates for Fennoscandia (mTC29) vary significantly among the three ecosystem models, mainly due to peatland extent. The peatland fractions in LPJG-WHyMe were determined mainly based on the hydrology scheme in Wania et al. (2009) and Granberg et al. (1999), whereas in LPX-Bern v1.0, the fraction is mainly based on the Northern Circumpolar Soil Carbon Database (NCSCD; Tarnocai et al., 2007). Due to a large peatland area, LPJG-WHyMe CH_4 emission estimates in Finland are about 10 times larger than the estimates from LPX-Bern-DYPTOP. For LPJG-WHyMe and LPX-Bern v1.0, it would theoretically be possible to use the same prescribed peatland extent distribution, but we used the reference versions which were already examined in the reference studies. Furthermore, their seasonal cycles show an

approximately 3 months difference in the timing of their summer maximum, even though all models use similar climate forcing data (CRU-TS datasets; 3.0 Mitchell and Jones (2005) for LPJG-WHyMe, and 3.21 dataset Harris et al. (2014) for LPX-Bern v1.0 and LPX-Bern-DYPTOP). A small sink of CH_4 in dry soil, estimated by each process model, is taken into account as negative biospheric fluxes. The global total annual sink to dry soil is estimated to be about 16–33% of the global total annual biospheric emissions in these process models. The percentage for Finland ranges considerably, from about 0.3% in LPJG-WHyMe to about 45% in LPX-Bern-DYPTOP on average. The emission estimates from rice were excluded from the biosphere estimates because these were already included in the EDGAR inventory. Although seasonality of the rice emissions could be significant for global emissions, rice is not cultivated in Finland. Biospheric emissions from water bodies (ocean, lakes and rivers) were neither taken into account in the prior nor optimized. With a relatively coarse model resolution and observation network, we did not expect the inversion to be able to constrain those emissions well. However, inland water emissions could have a significant contribution globally and also in northern high latitudes (Walter et al., 2006; Holgerson and Raymond, 2016; Thonat et al., 2017), since about 10%, 8% and 5% of the area of Finland, Sweden and Norway consists of water bodies, respectively, with inland water as a major contributor. Therefore, we must acknowledge the possible underestimation in our prior biospheric emission estimates from water bodies.

For monthly prior flux estimates from fire, the GFED v4.1 database was used, and for monthly ocean emissions, the estimates by Tsuruta et al. (2017) were applied. For termites, annual estimates from Ito and Inatomi (2012) were used as priors, and fixed year 2009 estimates for 2010–2014. The average 2004–2014 emissions of these sources for Finland were 0.18, 5.41, 0.95 Gg CH_4 yr^{-1} (i.e. 0.03%, 0.80%, 0.14% of total) for fire, termites and ocean, respectively. Note that these were not optimized because their source signals would be too small to be well constrained by the inversion. Other sources, such as natural geological emissions were not taken into account in this study. Although natural geological emissions are estimated to contribute to about 10% of global total emissions (Kirschke et al., 2013; Saunois et al., 2016), we know that these emissions are negligible for Finland (Etiope and Klusman, 2002).

2.3. Atmospheric CH_4 observations

In previous studies, the observations from Finland were limited to only one station at Pallas. Recently, an

Table 1. List of observations over Finland and surrounding regions.

Site code	Site name	Country	Contributor	Latitude [°N]	Longitude [°E]	Height* [m a.s.l.]	Obs. Unc. [ppb]	Date range** [mm/yyyy]
SMR	Hyytiälä	Finland	UHEL	61.85	24.28	306 (125)	25	11/2011–12/2014
KJN	Kjølnes	Norway	MPI&UE	70.85	29.24	30 (5)	15	10/2013–12/2014
KMP	Kumpula	Finland	FMI	60.20	24.96	53 (30)	30	5/2010–12/2014
PAL[†]	Pallas	Finland	FMI	67.97	24.12	572 (7)	15	2/2004–12/2014
PAL[†]	Pallas	Finland	NOAA	67.97	24.12	570 (7)	15	1/2004–12/2014
PUI	Puijo	Finland	FMI&UEF	62.91	27.66	316 (80)	30	6/20110–12/2014
SOD	Sodankylä	Finland	FMI	67.36	26.64	227 (48)	25	6/20128–12/2014
UTO	Utö	Finland	FMI	59.78	21.37	65 (57)	25	3/2012–12/2014

Observation Uncertainty (Obs. Unc.) is used to define diagonal values in the observation covariance matrix. This contains both measurement and model representativity error.

*Sampling heights from which atmospheric CH_4 is sampled in TM5. The numbers in the parenthesis are the measurement heights above ground.

**Date range for this study period, 2004–2014. Note that most of the observations are continuously updated, and measurements at Pallas (NOAA) started as early as in 2001.

[†]Observations from Pallas are coordinated by FMI and NOAA, of which NOAA observations are from discrete, and FMI observations are from continuous air samples.

extension of the observation network, made by the Finnish Meteorological Institute (FMI), the University of Eastern Finland (UEF), the University of Helsinki (UHEL), the Max-Planck-Institute for Biogeochemistry (MPI) and the University of Exeter (UE), was completed and the results became available for inversion studies. For a list of sites in the study region, see Table 1.

The Pallas site is a node of the Pallas-Sodankylä GAW station of the WMO/GAW monitoring network, located in Pallas-Yllästunturi National Park. It is a remote background station located on the treeless top of Sammaltunturi subarctic fell, measuring atmospheric carbon dioxide continuously since 1996 and CH_4 since 2004 by FMI. The site is surrounded by a mosaic of hills, coniferous forests and wetlands. Currently the measurements at Pallas, as well as at the other stations, are based on cavity ringdown spectroscopy (CRDS) instruments from Picarro Inc. (Santa Clara, CA), and the measurement set-up follows WMO/GAW protocol. The calibrations of FMI and UHEL sites are traceable to the WMO CH_4 X2004A scale. A detailed description of the Pallas-Sammaltunturi site, CH_4 observations and instrumentation is given in Aalto et al. (2007), Lohila et al. (2015) and Kilkki et al. (2015). Note that Hyytiälä is labelled as class 1 ICOS atmospheric station (since autumn 2017), Pallas is projected to be an ICOS class 1 station, and Puijo and Utö are going to be class 2 stations, and their measurement set-ups follow the ICOS protocols.

The Sodankylä measurements are made at the FMI Arctic Research Center, which is the other node of the Pallas,hents Aal GAW station. The measurements are made at a tower extending 48 m above ground, surrounded by sparse Scots pine forest. The station is surrounded by coniferous forests and wetlands, the closest

large fen being located 0.5 km away. Sodankylä town (8800 inhabitants, 2015) is 5 km from the measurement tower.

At the Puijo site, CH_4 is measured with a CRDS instrument (Picarro G2301) on the top of a telecommunication tower (Leskinen et al., 2009), which is located 2o3 km from the centre of Kuopio town (111,200 inhabitants, 2015). The tower (sampling point 84 m above ground) is built on a hill that is about 150 m above the surrounding lakes. Possible anthropogenic CH_4 sources include a waste landfill 10 km to the southwest, a wastewater treatment plant 5 km south-southeast, a district heating plant using a combination of peat, wood chips and heavy fuel oil as fuel 3 km south-southeast, and the tower itself (sewage ventilation) when the wind speed is low (< 2 m/s). In the sector from southwest to north, there are no significant anthropogenic CH_4 sources nearby.

Measurements at Kumpula are carried out in the roof of the FMI building at Helsinki (635,600 inhabitants, 2016). The sampling point is 30 m above the ground, and the building is located on a hill top about 24 m above sea level. The distance to the Baltic Sea shore is about one kilometre and it is about 4 km to the city centre. The site is located in a residential/commercial area, surrounded by parks, gardens and some major roads by the hill side. Similarly to Pallas, CH_4 is measured with a CRDS instrument, and the measurement set-up follows the WMO/GAW protocols (Kilkki et al., 2015).

The Utö site is located on an island in the Baltic Sea, about 80 km southwest of the Finnish mainland. It is a remote island about 1 km^2 in size, mostly rocky and treeless, with low grass and shrub vegetation and some tens of inhabitants mostly in summer. Measurements are

carried out from a cell phone mast at 57 m above ground and 65 m above sea level. A detailed description of the above mentioned FMI sites is given in Kilkki et al. (2015). Kilkki et al. (2015) focused on carbon dioxide, but the descriptions of the measurement set-ups mostly apply for CH_4 as well, since it is measured with the same CRDS instrument.

The Hyytiälä site is located in central Finland, in a wetland, forest, lake and agricultural landscape. There is an extensive wetland area 5 km from the site and a lake less than 1 km from the site. The CH_4 measurements are made from a mast 125 m above ground, surrounded mainly by coniferous forest. The CH_4 measurements, operated by the University of Helsinki, are based on CRDS instrumentation and connected to the same calibration scale as the FMI measurements, i.e. WMO/GAW standards. Details of the site are given in Keronen et al. (2014).

Kjølnes is a remote site in northernmost Norway at the Barents Sea coast, operated by the University of Exeter and the University of East Anglia. The measurement air intake is 30 m above ground. The landscape is treeless with bare rock and low grasses and sedges, and the closest village of Berlevåg is about 5 km away. CH_4 is measured with Off-Axis Integrated-Cavity Output Spectroscopy (Los Gatos Inc.), and the calibration scale as WMO CH_4 X2004A standards. The measurement precision is approximately 0.5 ppb, which is an average standard deviation of Target Tank measurements over the last 9-month period.

All observations were filtered before inversion to ensure a good spatial representativity of the measurements and to exclude instrumental errors. For FMI and UHEL observations, those with wind speed larger than 3 m/s and hourly standard deviation smaller than 4 ppb were chosen. For Kjølnes observations (MPI&UE), data were selected only by hourly standard deviation (< 4 ppb), and not by wind speed, as meteorological measurements were not available from the same location as that of atmospheric CH_4 measurements. For Pallas weekly sampled observations by National Oceanic and Atmospheric Administration (NOAA), those representing a large volume of air, i.e. spatially representative measurements were selected (flag starting with '.'). Due to the filtering, about 3–25% of observations were filtered out. From hourly observations, day time (12–16:00 local time) mean values were assimilated. Note that most of the observations presented here are not published, but all data is available on request to the authors.

For each site, observational uncertainty is defined based on site location and representativity of the transport model at each site (Tsuruta et al., 2017), and used in an observation error covariance matrix. The choice of observation uncertainty is somewhat arbitrary because there is no method to construct the observation error covariance matrix properly. However, our choice mostly lies within expected distributions (Michalak et al., 2005; Tsuruta et al., 2017). In this study, the observations were assumed uncorrelated over space and time; i.e. the observation error covariance matrix was diagonal. Observation uncertainties were also used as a rejection threshold. The observations were rejected in the assimilation if differences between observations and estimated mole fractions were three times the observational uncertainty. Note that we used predefined observation uncertainties that did not vary in time.

As CTE-CH_4 is a global model, we also used observations from the global WMO GAW network, available from the World Data Centre for Greenhouse Gas (WDCGG, data collected in April 2016). Among those, observations from other northern high latitudes, especially from the Eurasian boreal region, are important to constrain regional total emissions (Thompson et al., 2017). Since estimates for Finland are likely to be affected by surrounding regions, observations in Eurasian boreal regions have been also used in this study, similarly to Thompson et al. (2017). For global observations, uncertainties and rejection thresholds were assigned to each site in a similar way to those used in Finland, except for sites at high latitudes in the Southern Hemisphere (e.g. on Antarctica), where all observations were assimilated regardless of the estimated mole fractions, as in Tsuruta et al. (2017). For a list of global sites, see Supporting Information Table 1.

2.4. CH_4 surface flux measurements for evaluation

The seasonal cycle of the posterior flux estimates was evaluated against micrometeorological eddy covariance (EC) flux measurements from two wetland sites in Finland: Lompolojänkkä and Siikaneva. Note that the EC observations were not assimilated in the inversions.

Lompolojänkkä is an open mesotrophic sedge fen in northern Finland (67.60°N, 24.13°E, 269 m a.s.l., 5 km from Pallas-Sammaltunturi). The peat depth at Lompolojänkkä is about 2.5 m and almost the whole peat profile is water saturated throughout the year. The relatively dense vegetation layer is dominated by different sedges on the wet areas and different shrubs on relatively dry places. The moss cover is patchy with 57% coverage. The mean vegetation height on the fen is 40 cm with a maximum one-sided leaf area index (LAI) of 1.3.

Siikaneva is an open oligotrophic sedge fen, in southern Finland (61.50°N, 24.12°E, 162 m a.s.l., 5 km from Hyytiälä). The microtopography of the fen is relatively flat and the peat depth ranges from 2 m near the upland

Table 2. List of inversion setups.

Inversion	Prior [anthropogenic]	Prior [biospheric]	Observations	Period
J1	EDGAR v4.2 FT2010	LPX-Bern-DYPTOP	All available	2004–2014
J2	EDGAR v4.2 FT2010	LPX-Bern-DYPTOP	All but KMP and PUI	2010–2014
J3	EDGAR v4.2 FT2010	LPJG-WHyMe	All available	2010–2014
J4	EDGAR v4.2 FT2010	LPX-Bern v1.0	All available	2010–2014
J5	FIN-EDGAR	LPX-Bern-DYPTOP	All available	2010–2014

forest edge to almost 4 m at the centre of the site. The vegetation of the site is dominated by different sedges and a continuous Sphagnum carpet. A maximum one-sided LAI of 0.4 was observed for vascular plants in late July.

At both sites, the flux measurements were performed at a height of 3 m with similar instrumentation (3D anemometer (METEK) and different laser absorption spectrometry-based CH_4 analysers). The fluxes were processed to half-hourly values using block averaging and further calculated to monthly averages to enable comparison with model data. A detailed description of the measurement sites and systems are given in Aurela et al. (2009) and Aurela et al. (2015) for Lompolojänkkä and in Rinne et al. (2007) and Riutta et al. (2007) for Siikaneva.

2.5. Inversion setups

The list of inversion setups is presented in Table 2. In a reference inversion (J1), the prior flux estimates from EDGAR v4.2 FT2010 for anthropogenic and LPX-Bern-DYPTOP for biospheric sources were optimized, using all available observations from Finland and surrounding regions. In inversion J2, we examined the effect of urban observations by removing the Kumpula and Puijo observations. In inversions J3 and J4, we examine the effect of prior biospheric flux estimates by replacing LPX-Bern-DYPTOP estimates with those from LPJG-WHyMe and LPX-Bern v1.0 globally. In inversion J5, we examine the spatial distribution of anthropogenic emission estimates by replacing EDGAR v4.2 FT2010 with FIN-EDGAR estimates over Finland. When the observational constraints are large, we expect the inversion results to be close to each other regardless of the prior estimates.

3. Results

3.1. Atmospheric CH_4 at assimilated sites

Simulated posterior atmospheric CH_4 values at Finnish and surrounding sites generally correlate well with the observations ($r > 0.75$), but tend to have a negative bias (up to –7 ppb) (Fig. 1). The negative bias was especially prominent at Sodankylä when LPX-Bern-DYPTOP

estimates were used (J1, J2 and J5), although the correlation was high. The negative biases were improved at all sites, except at Kjølnes, in the inversion J3 where LPJG-WHyMe estimates were used. A similar improvement was also found for J4, where estimates from LPX-Bern v1.0 were used. This indicates that the inversion can match observations better when high prior emissions are used rather than low prior emissions (see Section 2.2). It can also be a sign of local wetland sources, because the bias is most pronounced in summer (Fig. 2). However, the bias at Kjølnes changed to positive and larger than J1, indicating the biospheric emissions in northern Finland may be overestimated by the inversions J3 and J4. In addition, those results may indicate that the correlation length of 500 km is too long for this region, and a shorter length is more appropriate. The distance between the Finnish and surrounding stations was about 150–300 km, i.e. biases could not be removed correctly with long correlation lengths. A test simulation with shorter correlation length (100 km) showed a better agreement with the observations. In that case, the biospheric emission estimates were larger than in J1 around Pallas, and anthropogenic emission estimates were larger than in J1 around Puijo. We acknowledge that a shorter correlation length gives more freedom in the inversion and the spatial distribution would be better resolved, and such set up could be encouraged for regional estimates. Most of the observations were assimilated in all inversions, and differences in the number of assimilated observations were insignificant between inversions.

The smallest RMSE was found at Kjølnes (max. 9 ppb), which is considered as a background site (Fig. 1). Despite discontinuity in the observation time series at Kjølnes, simulated CH_4 follows the observations well (Fig. 2). This confirms that the site could be considered as a good reference site for this region. Agreement with observations at Hyytiälä was also good; the bias being small ($< \pm 2$ ppb), the correlation high (>0.85), and the RMSE the second smallest among the eight sites (max. 12 ppb). In addition, one-to-one agreement (i.e. resulting the slope of the regression line) was closest to one among the new sites, after Pallas (Supporting Information Fig. 9). This indicates the advantage of the high-quality measurement design (e.g. air intake on a tall mast) and data at

those sites, which are possible reasons for the model to be able to resolve atmospheric CH_4 well. Therefore, Hyytiälä could also be a good reference site for future studies.

The weakest correlation and the largest RMSE were, as expected, found at Kumpula, highlighting the difficulty of estimating atmospheric CH_4 at sites in the middle of an area of local anthropogenic sources. Many of the summer peaks were not captured well in the model (Fig. 2). Even after data filtering, some observations influenced by local sources remained, and the model has difficulty in reproducing such high concentrations. With the FIN-EDGAR prior distribution (J5), the positive bias in the posterior CH_4 at Kumpula is reduced from about 1–2 ppb (J1, J3, J4) to –0.3 ppb (J5) (Fig. 1). Similar improvement was found at Puijo, where the bias improved from –4 ppb (J1) to –0.8 ppb (J5) (Fig. 1). These support our hypothesis that use of the FIN-EDGAR distribution is more favourable than the EDGAR distribution in a study with this focus.

3.2. Emission estimates

Average posterior total emissions for Finland for 2004–2014 are estimated to be 0.59 ± 0.51 Tg CH_4 yr^{-1}, with similar contributions from anthropogenic (0.31 ± 0.34 Tg CH_4 yr^{-1}) and biospheric (0.28 ± 0.22 Tg CH_4 yr^{-1}) sources (J1, mean weighted by number of observations from the sites in Finland and surrounding regions). The most significant transition from the prior to the posterior estimates is seen in summer and in 2010 (Figs. 3 and 4). The posterior biospheric emission over summer is higher than the LPX-Bern-DYPTOP estimate throughout the study period (Fig. 3). Increases in the emission estimates are somewhat expected, as peatland and wetland areas in this region are likely to be underestimated in LPX-Bern-DYPTOP, which could lead to smaller emission estimates (Stocker et al., 2014). In addition, this is consistent with a recent study by Thompson et al. (2017), which showed higher summer emissions over the Arctic and northern boreal regions than prior emissions mainly based on LPX-Bern-DYPTOP and EDGAR v4.2 FT2010 estimates.

The posterior total emission is higher than the prior before 2010, and lower after 2010, when significant changes occurred in anthropogenic emissions (Fig. 3). In 2010, assimilation of observations at Kumpula started. Since Kumpula is located near anthropogenic sources, such as the city of Helsinki, it is likely that the decrease in optimized anthropogenic emissions in 2010 was caused by assimilation of Kumpula observations. The hot-spot in the EDGAR inventory north of Helsinki is reduced to about half of the prior after 2010. Furthermore, the

seasonal cycle of anthropogenic emissions after 2010 is more pronounced than before 2010, showing high emissions during winter, and low during spring and autumn (Fig. 3). The anthropogenic cycle is opposite to that of biospheric emissions, which are larger during summer and lower during winter.

Although such a sudden change is unlikely to be realistic, significant changes have indeed taken place in landfill management over the recent years, and the Finnish national inventory shows a decrease in CH_4 emission estimates from 2004 to 2014 (Monni and Benviroc Ltd, 2013; Statistics Finland, 2015), indicating that the level of posterior emissions after 2010 is more reasonable than the level of the EDGAR inventory for the most recent years. Because the distribution in the EDGAR inventory is not consistent with the national inventory, the reported emission estimates could also be incorrectly distributed. In addition, we used the same prior for 2010–2014; i.e. the inter-annual variation in the prior is not well represented.

The uncertainty reduction ($1 - \sigma_{posterior}^2 / \sigma_{prior}^2$) is about 10 times higher in the biospheric emission estimates than in the anthropogenic emissions in Finland (Fig. 5, Supporting Information Figs. 11 and 12). In addition, the high uncertainty reduction around northern Finnish sites (Pallas and Sodankylä) is clear in biospheric emissions whereas no clear pattern is seen in that of anthropogenic emissions (Fig. 5). This is mainly due to prior state covariance structure (see Section 2.1), where biospheric emissions are assumed to be correlated between grid cells and anthropogenic emissions are assumed uncorrelated.

3.3. Sensitivity to observations

The anthropogenic emission estimates for Finland are very sensitive to observations from the urban measurement sites at Kumpula and Puijo. Inversion J2, without those sites, shows less significant decrease in the anthropogenic emission estimates after 2010 (Fig. 3), but large variations can be detected in emissions from late 2011 onward. Annual anthropogenic emissions are about 80% larger in J2 than in J1 (Table 3). The average annual emissions in J2 are even larger than the EDGAR inventory, although within the uncertainty that did not differ much between J1 and J5. Little influence of those sites was found for biospheric emissions, as expected (Fig. 3, Table 3).

The seasonal cycles of both anthropogenic and biospheric emission estimates were sensitive to observations from Kumpula and Puijo to some extent. High anthropogenic summer emissions were not seen in J1 in 2011, 2013, and 2014, whereas clear summer peaks were seen in J2 in all years (Fig. 3); i.e. those urban observations

removed the summer peaks. This suggests that the summer peaks in posterior anthropogenic emissions could have been driven by other observations such as Hyytiälä, Utö and Sodankylä, where measurements started in 2011–2012. Besides biospheric emissions, anthropogenic emissions of mainly agricultural origin occur near Hyytiälä. Utö and Sodankylä are far from significant anthropogenic sources, but they could capture some long range transported signals depending on air mass origins and trajectories. However, Hyytiälä observations have a gap in summer 2012 (from the end of June until the beginning of September), and in 2013 (from the beginning of May until the beginning of October), and Utö observations similarly have a gap between the end of February 2013 and mid-March 2014. Therefore, only Pallas and Sodankylä observations were assimilated in J2 during the summers of 2012 and 2013, when summer peaks were prominent. Sodankylä observations could be the main cause of the summer peaks, related to the high CH_4 values the model was not fully able to reproduce, but it cannot be confirmed based on the current results. Nevertheless, we suspect the summer peaks, caused by these observations, are probably more due to the biosphere than anthropogenic in origin. As the model has difficulties distinguishing the sources, posterior anthropogenic emissions are partly correlated with biospheric emissions, and some of the biospheric emissions might have been wrongly attributed to anthropogenic emissions.

3.4. Robustness with respect to the prior emission estimates

Previous studies showed that biospheric emissions estimated by process models are sensitive to model setups and inputs in northern high latitudes especially due to differences in the wetland extent applied (Wania et al., 2013), and inversion estimates depend on the prior estimates mostly in regions where limited observations are available (Bergamaschi et al., 2015; Thompson et al., 2017). Fennoscandia is one such region, where the uncertainty of the flux estimates is high in process-based ecosystem models. In this study, the average annual biospheric emission estimates for Finland for 2010–2014 from the three ecosystem models varied from 0.19 to 2.15 Tg CH_4 yr^{-1} in the prior, but the posterior estimates were more robust, ranging from 0.27 to 0.87 Tg CH_4 yr^{-1} (Table 3). The seasonal cycle is also more robust in the posterior than in the prior, especially for northern Finland around Lompolojänkkä (Fig. 4). However, the effect of the prior still remains for southern Finland around Siikaneva, possibly due to low prior uncertainty during summer in J1 (Fig. 4). The seasonal cycle of priors differs significantly around Siikaneva, mainly due to differences in the extent of peatlands. The average area fraction of peatland around

Siikaneva is about 0.5% in LPX-Bern-DYPTOP, and about 9% in LPX-Bern v1.0. The seasonal cycle of CH_4 fluxes in LPX-Bern-DYPTOP is therefore strongly affected by fluxes from another soil type (wetsoil). Although Siikaneva is a relatively large peatland, there are also agricultural and anthropogenic fields in its surroundings, and anthropogenic emissions in the prior are larger than the biospheric emissions. Therefore, the inversion is likely to increase summer emissions from anthropogenic sources rather than the biospheric sources (see Section 4.2). In addition, winter estimates (November–February) follow the prior closely. Although the differences are small, the posterior estimates do not perfectly agree with one another. Winter biospheric emission is assumed to be small, as most of Finland is covered by snow and soil temperature drops to below freezing (0°C). Observations near biospheric sources therefore capture little of the biospheric signals during winter.

The spatial distribution also depends on the prior despite the grid-based inversion. Average annual emission of LPX-Bern v1.0 (J4) in Finland is smaller than that of LPJG-WHyMe (J3), but the posterior estimates in J3 are smaller than in J4 (Table 3). Both inversions showed significant decrease in emission estimates in southern Finland, but the estimates in J3 decreased more than in J4 in northern Finland, where J4 estimates remained high around Pallas (Supporting Information Fig. 12). This is mostly because of differences in the prior distribution north of Pallas, where LPJG-WHyMe has high emissions up to Kjølnes (nearly 71°N) and LPX-Bern v1.0 has high emissions only up to about 68°N. The uncertainty reduction also shows higher reduction in J3 around Pallas than in J4 (Supporting Information Fig. 12). This suggests that the inversions were trying to conserve the budget in this region, but did not know exactly where to place the emissions, and thus followed the prior distribution. This also indicates the large influence of the Pallas observations on emissions far to the north.

To make the estimates more robust, a higher prior uncertainty (especially when emission estimates are low) and higher weights on observations (i.e. smaller observation uncertainty) could be assigned. Indeed, the J1 posterior uncertainty is much smaller than that of J3 and J4, and the low uncertainty of J1 might be an underestimation. For observations such as from Hyytiälä and Utö, posterior RMSE (< 18 ppb) is smaller than observation uncertainty (25 ppb), indicating that the model was able to produce atmospheric CH_4 better than our prior expectation, and therefore we could assume a smaller observational uncertainty for those sites.

Compared to J1, using the EDGAR v4.2 FT2010 inventory, J5 estimates using the FIN-EDGAR inventory have higher anthropogenic emissions in central Finland and lower in southern Finland, which is strongly inherited from prior emissions (Fig. 5). In J5, regional total posterior
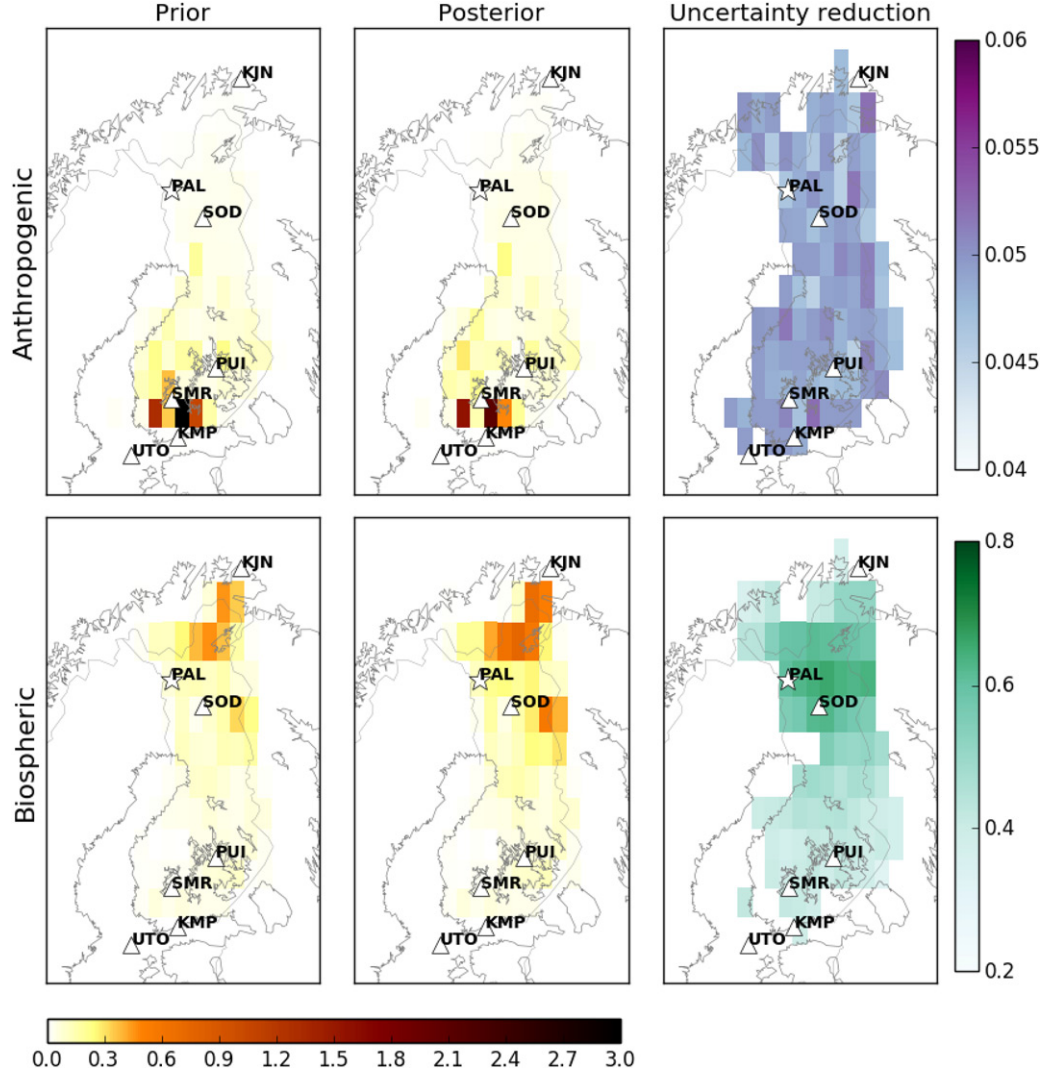
Fig. 5. Mean annual emission estimates for 2010–2014 [10^{-8} mol m^{-2} s^{-1}], their uncertainty reduction ($1 - \sigma^2_{\text{posterior}} / \sigma^2_{\text{prior}}$), and locations of observations in Fennoscandia. The triangles show sites with continuous observations and the star shows the site with both continuous and discrete observations. For other inversions, see Supplementary Material.

anthropogenic emissions are slightly higher than the prior, again showing an increase in central Finland, where the emissions from agricultural activities are large. Little difference between prior and posterior emissions was found for southern Finland, supporting the FIN-EDGAR distribution rather than the EDGAR distribution. However, the J5 posterior annual anthropogenic emissions are much greater than estimated by the national inventory, indicating a possible problem in the inversion. We must acknowledge that the separation of biospheric and anthropogenic emissions is still very uncertain, and the high anthropogenic estimates may not actually be anthropogenic sources. The long correlation length would also have caused the difficulties in source separation, especially in the southern part of Finland. For example, the Kumpula observations capture signals mainly from local

anthropogenic sources, but affect emission estimates up to 500 km around the site, i.e. the observations could influence the emission estimates in the middle of Finland, where biospheric sources are dominant. This suggests shorter correlation length (e.g. 100 km) is more appropriate for observations in middle to southern Finland.

3.5. Evaluation of emission estimates

Biospheric emission estimates were compared to the micrometeorological eddy covariance (EC) flux observations from Lompolojänkkä and Siikaneva. For the comparison, regional mean estimates were calculated from model grids around the sites, $\pm i^\circ$ latitudinal bands inside the Finnish border.

Compared to the EC observations, the posterior matches the flux observations better than the prior, and the posterior estimates are more robust than the prior (Fig. 4). In terms of magnitude, reductions from LPJG-WHyMe and LPX-Bern v1.0 and increases from LPX-Bern-DYPTOP led to a better agreement with the observed fluxes, although the posterior emissions are still slightly higher than observed fluxes at Lompolojänkkä (Fig. 4). Inter-annual variability is especially strong in LPX-Bern v1.0, with exceptionally high CH_4 emissions in 2004, 2006 and 2011. There are several possible explanations for those high emission estimates. In 2004, the wet soil emission estimate was high, and in 2006, the peatland emission estimate was high. In 2011, all (inundated, wet soil and peatland) emissions were relatively high compared to other years, which led to high estimates overall. However, since we did not find significant inter-annual variability in the source area extent of inundated and wet soil areas, this is more due to climate drivers, such as temperature and precipitation. Such strong inter-annual variability was not seen in the EC observations, and the inter-annual variability does not always agree with EC measurements. For example, the measurements do not show high peatland emission in 2006. Rather, it was low, as 2006 was an exceptionally dry year.

Some years, such as 2007 show high emission from Lompolojänkkä during spring, and the posterior successfully increased the estimates from the prior. This suggests that the high emission signal was possibly captured by the atmospheric CH_4 observations at Pallas, indicating that the high CH_4 originated from large emission areas. Long-lasting precipitation periods, like in summer-autumn 2011, may also indicate a CH_4 source in forested upland soils (Lohila et al., 2016), where the emitting area is very large, and thus the atmospheric observations see elevated CH_4, further increasing emission estimates.

The seasonal cycle shows that the summer maximum in LPX-Bern-DYPTOP is well captured around Lompolojänkkä, but generally a month later than in the EC observations around Siikaneva (Fig. 4). The inversion also fails to capture the seasonal cycle around Siikaneva well when using LPX-Bern-DYPTOP as a prior. For Siikaneva, the posterior estimates from J4 matched the EC observations best, where the seasonal cycle of the prior (LPX-Bern v1.0) also matched the observations best among the priors (Fig. 4). The seasonal cycle in J3 is also better captured than in J1, but the magnitude of the seasonal maximum is much smaller than in J4, which is again inherited from the prior (LPJG-WHyMe).

However, although the Pallas-Sammaltunturi is close to Lompolojänkkä, the Pallas atmospheric observations do not adequately capture local signals from Lompolojänkkä, which is a relatively small wetland, but

Table 3. Average annual CH_4 emission estimates between 2010 and 2014 in Finland [Tg CH_4 yr^{-1}].

	Anthropogenic	Biosphere
(Prior)		
EDGAR v4.2 FT2010	0.39	
FIN-EDGAR	0.38	
LPX-Bern-DYPTOP		0.19
LPJG-WHyMe		2.15
LPX-Bern v1.0		1.29
(Posterior)		
J1	0.27 ± 0.34	0.27 ± 0.23
J2	0.41 ± 0.34	0.27 ± 0.23
J3	0.19 ± 0.34	0.73 ± 1.43
J4	0.20 ± 0.34	0.87 ± 1.02
J5	0.44 ± 0.33	0.26 ± 0.22

rather capture signals from a larger area (Aalto et al., 2007). This is probably one of the reasons why some exceptional seasonal cycles were not well captured in the posterior. For example, a spring boost of CH_4 emission in 2009 is seen in Lompolojänkkä observations, which is possibly because a substantial amount of CH_4 was stored in snow and below ice in winter and released during the snow melt. Both prior and posterior fluxes fail to see this feature, although posterior estimates are slightly higher than the prior. This could possibly be improved by increasing prior uncertainty during spring to allow more freedom in the optimization. Furthermore, storage of CH_4 in frozen soils and snow could be added to future versions of ecosystem models used for prior estimates.

Although the average fluxes of larger areas are not directly comparable with site-level observations such that emission magnitudes from the site observations may not be representative of large area averages, we assume that Lompolojänkkä and Siikaneva represent general characteristics of wetlands in northern and southern Finland, respectively. In addition, with current CTE-CH_4, a regional average would be more appropriate for the comparison than the estimates from a single grid point because the observation network and the optimization resolution are not dense enough for a site-level comparison. Nevertheless, the comparison can provide useful information for further development.

4. Discussion

4.1. Spatial representativity of observations

Most of the observations in Finland capture not only local signals, but also those come from, e.g. the Atlantic Ocean, western Russia or even from central Europe (Aalto et al., 2007; Kilkki et al., 2015). A good spatial representativity of the observations is shown especially

from the Pallas site. This is an advantage of the site location, which is on top of the Sammaltunturi subarctic fell with small local CH_4 sources, and far from anthropogenic sources. On the other hand, other observations, especially from urban sites, might be difficult to use in large scale regional inversion studies. In this study, we used two urban sites: Kumpula and Puijo, where Kumpula is located near the centre of Helsinki city, and Puijo is located near the city of Kuopio. Some of these urban observations capture strong local signals, mainly from anthropogenic sources (Kilkki et al., 2015). Such observations could affect regional inversion estimates, resulting in a possible overestimation of emission estimates due to low spatial representativity of these observations in comparison to the model grid size. In this study, the hourly observations were filtered based on wind speed and measurement standard deviation within each hour to select observations at well-mixed atmospheric conditions. However, a better criteria should be used, e.g. from detailed flags where are available, as the wind speed only cannot fully define atmospheric conditions. In addition, the observations that differ significantly from model estimates were rejected (three times observation uncertainty, see Section 2.3). However, we acknowledge that some observations unrepresentative of large scale conditions could still have been assimilated in the inversions.

Nevertheless, the analysis of posterior atmospheric CH_4 and the spatial correlations of posterior emissions suggest that the assimilated urban observations are acceptable for use in inversion studies. Observations from Kumpula seem to influence the emission estimates of near-by model grid cells. This is partly due to the applied covariance structure (prior emissions on near-by grid cells are assumed correlated in space), but also due to influence by the observations. For Puijo, the observations seem to be less representative for large areas, but due to relatively small emissions around the site, the influence on estimated country total emissions was small.

Although the observation network used in the inversions is substantially extended, additional observations in central Finland and in neighbouring countries would be needed to better constrain emissions in Finland and neighbouring countries. The observations from north, west and south directions is continuously increasing and will be available from, e.g. the ICOS network.

4.2. Seasonal cycle of anthropogenic and biospheric emissions in Finland

The seasonal cycle of anthropogenic emissions is more pronounced after 2010 than before 2010. The inversion estimates before 2010 are likely affected by surrounding regions, such as western Russia and central Europe. Since Pallas is far from anthropogenic sources, inversions cannot optimize anthropogenic emissions based on local observations before 2010. The emission estimates after 2010 show two peaks, one during winter (Dec.–Feb.) and one during summer (May–Jul.). Although anthropogenic emissions are argued to have little seasonal variability, summer peaks may indicate high anthropogenic emission sources in Finland that are mainly from agriculture and landfills. Winter peaks may reflect emissions from, e.g. heating by burning biomass fuels, which is expected to be higher during winter.

However, we did not find independent evidence to support such seasonal variability in anthropogenic emissions. The winter emission peaks did not correlate well with winter temperature for example, which could be explained by heating emissions. In addition, the two peaks are also found in inversion J2, where observations from city sites were excluded. Therefore, the seasonal cycle in the anthropogenic emission estimates was not reflected from observations from urban sites, such as those from Kumpula and Puijo, although one would expect that urban observations are most strongly influenced by a potential seasonal signal of anthropogenic emissions. This suggests that the seasonal cycle in anthropogenic emissions inferred by the inversion does not reflect reality, but resulted from correlation with biospheric emission estimates.

4.3. Contribution of emissions from Finland and Fennoscandia to other high Northern latitude and global estimates

Total posterior CH_4 emissions from Finland are about 26 to 28% of Fennoscandian (mTC29) emissions, except for J4 (LPX-Bern v1.0 as prior), in which Finland contributed to about 42% of Fennoscandian emissions (Supporting Information). The posterior biospheric emissions in Finland are the highest in J4 among the inversions, which resulted in the high share in the Fennoscandian emissions (see Section 3.4). The emission shares of Finland found in the inversions are mainly inherited from the prior biospheric emissions. The contribution of biospheric emission in Finland to Fennoscandia is lower in LPX-Bern-DYPTOP (32%) and LPJG-WHyMe (37%) compared to LPX-Bern v1.0 (54%). This again shows that the inversion is not able to completely resolve inconsistencies in the prior spatial distributions.

The contribution of estimated total Fennoscandian emissions is only about 0.4% of the global total emission estimate of 534 ± 84 Tg CH_4 yr^{-1} in J1 for 2010–2014. Flux estimates, including their inter-annual variability, seasonal cycle, and spatial distribution outside Fennoscandia are hardly affected by the different priors

and observations used in the different inversion setups in this study. Although global total emissions increased during 2004–2014 from 510 ± 73 to 540 ± 84 Tg CH_4 yr^{-1}, neither prior nor posterior emissions suggest a contribution to global increase from Fennoscandia. Globally, the increasing trend may be overestimated as we did not consider inter-annual variability and potential trends in photochemical reaction rates with OH (Rigby et al., 2008, 2017; Montzka et al., 2011; McNorton et al., 2016; Turner et al., 2017). As our inversion results depend on atmospheric CH_4 observations, it is important to account correctly for the atmospheric CH_4 sinks. However, we assume that uncertainty in emission estimates are larger than in sinks, and we cannot separately estimate the emissions and the local atmospheric CH_4 sink in Fennoscandia.

CH_4 emissions over Finland and Fennoscandia estimated by our grid-based inversions are comparable to those found in regional-based optimizations where either biospheric or anthropogenic fluxes per region are optimized (Tsuruta et al., 2017). The grid-based inversions yield only about 4% lower biospheric emissions than the region-based inversion and both show an increase in biospheric emissions from the prior (LPX-Bern-DYPTOP). For anthropogenic emissions, the estimates for Finland in both cases show a decrease from the prior. Both cases also show a decrease from the prior for the anthropogenic emissions in Fennoscandia, but the decrease is much stronger in the grid-based inversion than in the regional-based inversion (about 36% and 12% reductions from the priors, respectively). This suggests that the effect of observations from the urban sites on emission estimates is stronger in the grid-based inversion. In addition, the regional inversions could be affected more strongly by observations outside Fennoscandia, and correlation with nearby regions could be higher. An increase in western Russian anthropogenic emissions therefore, could compensate for the decrease of the Fennoscandian emissions in a regional inversion. Although it was not possible to perform a global grid-based inversion due to computational limitations, the comparison shows the advantage of grid-based inversions in regions with sufficiently dense observations.

5. Summary

We estimated the methane budget in Finland for 2004–2014 using the CTE-CH_4 data assimilation system. In this study, the atmospheric CH_4 observations from seven sites in Finland and surrounding regions were assimilated: Hyytiälä, Kjølnes, Kumpula, Pallas, Puijo, Sodankylä and Utö. Comparison with posterior atmospheric CH_4 showed good agreement with the observations from those sites, indicating that the model is able to resolve atmospheric CH_4 at those sites well, and that the observations can be used in future atmospheric inversion studies. The urban sites Kumpula and Puijo are also useful in inversion studies after careful data filtering. However, new regionally representative sites would be needed especially in the middle part of Finland to reliably constrain the national methane budget. The posterior biospheric emissions were more robust than the priors, especially for Northern Finland, and captured independent CH_4 flux measurements from Lompolojänkkä reasonably well. Although the grid size of the model is still much larger than the footprint of flux measurements, this indicated the advantages of small scale ($1° \times 1°$ in this case) optimization. In addition, the inversion was able to reduce biospheric emission uncertainty estimates by about 40–80% per model grid. Our inversion showed that, compared to the inversion using original EDGAR inventory, the inversion using an adjusted prior that redistributed the EDGAR national totals based on the national inventory showed improved results. The spatial distribution of the anthropogenic emissions is difficult to constrain well with the current inversion setups, so we would like to raise the point that a reliable prior distribution when available, should be used in inversion studies. The estimated contribution of emissions from Finland to global emissions was only about 0.13%, and our results showed no increasing trend in the emissions from Finland suggesting that they have not contributed to an increase in global emissions.

University of Malta, University of Urbino, Centre for Environmental Monitoring (RIVM), Institute of Atmospheric Sciences and Climate, Ricerca sul Sistema Energetico (RSE SpA), and Chinese Academy of Meteorological Sciences (CMA) for performing high-quality CH_4 measurements at global sites and making them available through the GAW-WDCGG. The observations by J.M.A. are a part of the GAW program of the WMO. We also appreciate Statistics Finland for developing and publishing national inventory data available for scientific research.

Disclosure statement

No potential conflict of interest was reported by the authors.

Funding

Supplemental data

Supplemental data for this article can be accessed here https://doi.org/10.1080/16000889.2018.1565030.

References

Aalto, T., Hatakka, J. and Lallo, M. 2007. Tropospheric methane in northern Finland: seasonal variations, transport patterns and correlations with other trace gases. *Tellus B.* **59**, 251–259. doi:10.1111/j.1600-0889.2007.00248.x.

Aurela, M., Lohila, A., Tuovinen, J.-P., Hatakka, J., Riutta, T. and co-authors. 2009. Carbon dioxide exchange on a northern boreal fen. *Boreal Environ. Res.* **14**, 699–710.

Aurela, M., Lohila, A., Tuovinen, J.-P., Hatakka, J., Penttilä, T. and co-authors. 2015. Carbon dioxide and energy flux measurements in four northern-boreal ecosystems at Pallas. *Boreal Environ. Res.* **20**, 455–473.

Bergamaschi, P., Krol, M., Dentener, F., Vermeulen, A., Meinhardt, F. and co-authors. 2005. Inverse modelling of national and European CH_4 emissions using the atmospheric zoom model TM5. *Atmos. Chem. Phys.* **5**, 2431–2460. doi: 10.5194/acp-5-2431-2005.

Bergamaschi, P., Corazza, M., Karstens, U., Athanassiadou, M., Thompson, R. L. and co-authors. 2015. Top-down estimates of European CH_4 and N_2O emissions based on four different inverse models. *Atmos. Chem. Phys.* **15**, 715–736. doi:10.5194/acp-15-715-2015.

Bergamaschi, P., Karstens, U., Manning, A. J., Saunois, M., Tsuruta, A. and co-authors. 2018. Inverse modelling of European CH_4 emissions during 2006uropean CH.519fferent inverse models and reassessed atmospheric observations. *Atmos. Chem. Phys.* **18**, 901–920.

Bousquet, P., Ringeval, B., Pison, I., Dlugokencky, E. J., Brunke, E.-G. and co-authors. 2011. Source attribution of the changes in atmospheric methane for 2006–2008. *Atmos. Chem. Phys.* **11**, 3689–3700.

Brühl, C. and Crutzen, P. J. 1993. MPIC Two-dimensional model. *NASA Ref. Publ.* **1292**, 103–104.

Bruhwiler, L., Dlugokencky, E., Masarie, K., Ishizawa, M., Andrews, A. and co-authors. 2014. CarbonTracker-CH_4: an assimilation system for estimating emissions of atmospheric methane. *Atmos. Chem. Phys.* **14**, 8269–8293.

Christensen, T. R., Prentice, I. C., Kaplan, J., Haxeltine, A. and Sitch, S. 1996. Methane flux from northern wetlands and tundra. *Tellus B.* **48**, 652–661.

Christensen, T. R., Ekberg, A., Ström, L., Mastepanov, M., Panikov, N. and co-authors. 2003. Factors controlling large scale variations in methane emissions from wetlands. *Geophys. Res. Lett.* **30**, 1414.

Ciais, P., Sabine, C., Bala, G., Bopp, L., Brovkin, V. and co-authors. 2013. Carbon and other biogeochemical cycles. In: Climate Change 2013: The Physical Science Basis. Contribution of Working Group I to the Fifth Assessment Report of the Intergovernmental Panel on Climate Change (ed. T. F. Stocker, D. Qin, G.-K. Plattner, M. Tignor, S. K. Allen, and co-authors). Technical report. Cambridge University Press, Cambridge. https://www.ipcc.ch/pdf/assessment-report/ar5/wg1/WG1AR5_Chapter08_FINAL.pdf.

Cresto Aleina, F., Runkle, B. R. K., Brücher, T., Kleinen, T. and Brovkin, V. 2016. Upscaling methane emission hotspots in boreal peatlands. *Geosci. Model Dev.* **9**, 915–926.

Dinsmore, K. J., Drewer, J., Levy, P. E., George, C., Lohila, A. and co-authors. 2017. Growing season CH_4 and N_2O fluxes from a subarctic landscape in northern Finland; from chamber to landscape scale. *Biogeosciences* **14**, 799–815.

EDGAR. 2010. *Emission Database for Global Atmospheric Research (EDGAR), Release Version 4.2 FT2010*. http://edgar.jrc.ec.europa.eu.

Emmerton, C. A., St. Louis, V. L., Lehnherr, I., Graydon, J. A., Kirk, J. L. and co-authors. 2016. The importance of freshwater systems to the net atmospheric exchange of carbon dioxide and methane with a rapidly changing high Arctic watershed. *Biogeosciences* 13, 5849–5863.

Etiope, G. and Klusman, R. W. 2002. Geologic emissions of methane to the atmosphere. *Chemosphere* 49, 777–789.

Fisher, R. E., France, J. L., Lowry, D., Lanoisellé, M., Brownlow, R. and co-authors. 2017. Measurement of the ^{13}C isotopic signature of methane emissions from Northern European wetlands. *Global Biogeochem. Cycles* 31, 605–623.

Frolking, S. and Crill, P. 1994. Climate controls on temporal variability of methane flux from a poor fen in southeastern New Hampshire: Measurement and modeling. *Global Biogeochem. Cycles* 8, 385–397.

GEA. 2012. *Global Energy Assessment - Toward a Sustainable Future*. International Institute for Applied Systems Analysis. Vienna, Austria and Cambridge University Press, Cambridge, UK and New York, NY, USA.

Granberg, G., Grip, H., Löfvenius, M. O., Sundh, I., Svensson, B. H. and co-authors. 1999. A simple model for simulation of water content, soil frost, and soil temperatures in boreal mixed mires. *Water Resour. Res.* 35, 3771–3782.

Gregory, D., Morcrette, J.-J., Jakob, C., Beljaars, A. C. M. and Stockdale, T. 2000. Revision of convection, radiation and cloud schemes in the ECMWF integrated forecasting system. *QJR. Meteorol. Soc.* 126, 1685–1710.

Harris, I., Jones, P., Osborn, T. and Lister, D. 2014. Updated high-resolution grids of monthly climatic observations – the CRU TS3.10 dataset. *Int. J. Climatol.* 34, 623–642.

Hofmann, D. J., Butler, J. H., Dlugokencky, E. J., Elkins, J. W., Masarie, K. and co-authors. 2006. The role of carbon dioxide in climate forcing from 1979 to 2004: introduction of the Annual Greenhouse Gas Index. *Tellus B.* 58, 614–619.

Holgerson, M. A. and Raymond, P. A. 2016. Large contribution to inland water CO_2 and CH_4 emissions from very small ponds. *Nature Geosci.* 9, 222–226.

Houweling, S., Krol, M., Bergamaschi, P., Frankenberg, C., Dlugokencky, E. J. and co-authors. 2014. A multi-year methane inversion using SCIAMACHY, accounting for systematic errors using TCCON measurements. *Atmos. Chem. Phys.* 14, 3991–4012.

Houweling, S., Kaminski, T., Dentener, F., Lelieveld, J. and Heimann, M. 1999. Inverse modeling of methane sources and sinks using the adjoint of a global transport model. *J. Geophys. Res.* 104, 26137–26160.

Huttunen, J. T., Nykänen, H., Turunen, J. and Martikainen, P. J. 2003. Methane emissions from natural peatlands in the northern boreal zone in Finland, Fennoscandia. *Atmos. Environ.* 37, 147–151.

Ito, A. and Inatomi, M. 2012. Use of a process-based model for assessing the methane budgets of global terrestrial ecosystems and evaluation of uncertainty. *Biogeosciences* 9, 759–773.

Keronen, P., Reissell, A., Siivola, E., Vesala, T., Pohja, T. and co-authors. 2014. Accurate measurements of CO_2 mole fraction in the atmospheric surface layer by an affordable instrumentation. *Boreal Environ. Res.* 19, 35–54.

Kilkki, J., Aalto, T., Hatakka, J., Portin, H. and Laurila, T. 2015. Atmospheric CO_2 observations at Finnish urban and rural sites. *Boreal Environ. Res.* 20, 227–242.

Kirschke, S., Bousquet, P., Ciais, P., Saunois, M., Canadell, J. G. and co-authors. 2013. Three decades of global methane sources and sinks. *Nat. Geosci.* 6, 813–823.

Krol, M., Houweling, S., Bregman, B., van den Broek, M., Segers, A. and co-authors. 2005. The two-way nested global chemistry-transport zoom model TM5: Algorithm and applications. *Atmos. Chem. Phys.* 5, 417–432.

Lerner, J., Matthews, E. and Fung, I. 1988. Methane emission from animals: A global high-resolution data base. *Global Biogeochem. Cycle.* 2, 139–156.

Leskinen, A., Portin, H., Komppula, M., Miettinen, P., Arola, A. and co-authors. 2009. Overview of the research activities and results at Puijo semi-urban measurement station. *Boreal Environ. Res.* 14, 576–590.

Lohila, A., Minkkinen, K., Aurela, M., Tuovinen, J.-P., Penttilä, T. and co-authors. 2011. Greenhouse gas flux measurements in a forestry-drained peatland indicate a large carbon sink. *Biogeosciences* 8, 3203–3218.

Lohila, A., Penttilä, T., Jortikka, S., Aalto, T., Anttila, P. and co-authors. 2015. Preface to the special issue on integrated research of atmosphere, ecosystems and environment at Pallas. *Boreal Environ. Res.* 20, 431–454.

Lohila, A., Aalto, T., Aurela, M., Hatakka, J., Tuovinen, J.-P. and co-authors. 2016. Large contribution of boreal upland forest soils to a catchment-scale CH_4 balance in a wet year. *Geophys. Res. Lett.* 43, 2946–2953.

McGuire, A. D., Christensen, T. R., Hayes, D., Heroult, A., Euskirchen, E. and co-authors. 2012. An assessment of the carbon balance of Arctic tundra: Comparisons among observations, process models, and atmospheric inversions. *Biogeosciences* 9, 3185–3204.

McNorton, J., Chipperfield, M. P., Gloor, M., Wilson, C., Feng, W. and co-authors. 2016. Role of OH variability in the stalling of the global atmospheric CH_4 growth rate from 1999 to 2006. *Atmos. Chem. Phys.* 16, 7943–7956.

Michalak, A. M., Hirsch, A., Bruhwiler, L., Gurney, K. R., Peters, W. T. and co-authors. 2005. Likelihood estimation of covariance parameters for Bayesian atmospheric trace gas surface flux inversions. *J. Geophys. Res.* 110. doi:10.1029/2005JD005970.

Minkkinen, K., Korhonen, R., Savolainen, I. and Laine, J. 2002. Carbon balance and radiative forcing of Finnish peatlands 1900–2100 – The impact of forestry drainage. *Global Change Biol.* 8, 785–799.

Mitchell, T. D. and Jones, P. D. 2005. An improved method of constructing a database of monthly climate observations and associated high-resolution grids. *Int. J. Climatol.* 25, 693–712.

Monni, S. and Benviroc Ltd. 2013. Finland's Sixth National Communication under the United Nations Framework Convention on Climate Change. Technical report. Ministry of

the Environment and Statistics Finland, Helsinki, 314 pp. https://www.stat.fi/tup/khkinv/fi_ nc6.pdf.

Monteil, G., Houweling, S., Butz, A., Guerlet, S., Schepers, D. and co-authors. 2013. Comparison of CH_4 inversions based on 15 months of GOSAT and SCIAMACHY observations. *J. Geophys. Res. Atmos.* **118**, 11807–11823.

Montzka, S. A., Krol, M., Dlugokencky, E., Hall, B., Jockel, P. and co-authors. 2011. Small interannual variability of global atmospheric hydroxyl. *Science* **331**, 67–69.

Moore, T. R., Heyes, A. and Roulet, N. T. 1994. Methane emissions from wetlands, southern Hudson Bay lowland. *J. Geophys. Res.* **99**, 1455–1467.

Moore, T. R., Roulet, N. T. and Waddington, J. M. 1998. Uncertainty in predicting the effect of climatic change on the carbon cycling of Canadian peatlands. *Climatic Change* **40**, 229–245.

Nykänen, H., Alm, J., Silvola, J., Tolonen, K. and Martikainen, P. J. 1998. Methane fluxes on boreal peatlands of different fertility and the effect of long-term experimental lowering of the water table on flux rates. *Global Biogeochem. Cycles* **12**, 53–69.

Olivier, J. and Janssens-Maenhout, G. 2012. *CO2 Emissions from Fuel Combustion. 2012 ed. Part III: Greenhouse-Gas Emissions*. OECD Publishing, Paris. https://www.pbl.nl/en/publications/2012/co2-emissions-from-fuel-combustion-2012-edition.

Peters, W., Miller, J. B., Whitaker, J., Denning, A. S., Hirsch, A. and co-authors. 2005. An ensemble data assimilation system to estimate CO_2 surface fluxes from atmospheric trace gas observations. *J. Geophys. Res.* **110**, D24304.

Petrescu, A. M. R., van Beek, L. P. H., van Huissteden, J., Prigent, C., Sachs, T. and co-authors. 2010. Modeling regional to global CH_4 emissions of boreal and arctic wetlands. *Global Biogeochem. Cycles* **24**, GB4009.

Ravela, S. and McLaughlin, D. 2007. Fast ensemble smoothing. *Ocean Dyn.* **57**, 123–134.

Rigby, M., Prinn, R. G., Fraser, P. J., Simmonds, P. G., Langenfelds, R. L. and co-authors. 2008. Renewed growth of atmospheric methane. *Geophys. Res. Lett.* **35**, L22805.

Rigby, M., Montzka, S. A., Prinn, R. G., White, J. W. C., Young, D. and co-authors. 2017. Role of atmospheric oxidation in recent methane growth. *Proc. Natl. Acad. Sci. USA* **114**, 5373–5377.

Rinne, J., Riutta, T., Pihlatie, M., Aurela, M., Haapanala, S. and co-authors. 2007. Annual cycle of methane emission from a boreal fen measured by the eddy covariance technique. *Tellus B.* **59**, 449–457.

Riutta, T., Laine, J., Aurela, M., Rinne, J., Vesala, T. and co-authors. 2007. Spatial variation in plant community functions regulates carbon gas dynamics in a boreal fen ecosystem. *Tellus B.* **59**, 838–852.

Saunois, M., Bousquet, P., Poulter, B., Peregon, A., Ciais, P. and co-authors. 2016. The global methane budget 2000.x.11. *Earth Syst. Sci. Data* **8**, 697–751.

Schaefer, H., Fletcher, S. E. M., Veidt, C., Lassey, K. R., Brailsford, G. W. and co-authors. 2016. A 21st-century shift from fossil-fuel to biogenic methane emissions indicated by 13CH4. *Science* **352**, 80–84.

Schwietzke, S., Sherwood, O. A., Bruhwiler, L. M. P., Miller, J. B., Etiope, G. and co-authors. 2016. Upward revision of global fossil fuel methane emissions based on isotope database. *Nature* **538**, 88–91.

Smith, B., Prentice, I. C. and Sykes, M. T. 2001. Representation of vegetation dynamics in the modelling of terrestrial ecosystems: comparing two contrasting approaches within European climate space. *Global Ecol. Biogeogr.* **10**, 621–637. 2001.t01-1-00256.x.

Spahni, R., Joos, F., Stocker, B. D., Steinacher, M. and Yu, Z. C. 2013. Transient simulations of the carbon and nitrogen dynamics in northern peatlands: From the last glacial maximum to the 21st century. *Clim. Past* **9**, 1287–1308.

Statistics Finland. 2015. *Finland's Second Biennial Report under the UNFCCC*. Technical report. Ministry of the Environment and Statistics Finland. 82 pp. https://unfccc.int/files/national_reports/biennial_reports_and_iar/submitted_biennial_reports/application/pdf/fi_br2_tk_20151217_final.pdf.

Statistics Finland PX-Web regional database. n.d. *Regional Greenhouse Gas Emissions, Data on Non-Emissions Trading Scheme by Region, Emission Category, Year and Data.* http://pxnet2.stat.fi/PXWebPXWeb/pxweb/fi/StatFin/StatFin__ymp__khki/020_khki_tau_102.px/.

Stocker, B. D., Spahni, R. and Joos, F. 2014. DYPTOP: A cost-efficient TOPMODEL implementation to simulate sub-grid spatio-temporal dynamics of global wetlands and peatlands. *Geosci. Model Dev.* **7**, 3089–3110.

Stohl, A., Aamaas, B., Amann, M., Baker, L. H., Bellouin, N. and co-authors. 2015. Evaluating the climate and air quality impacts of short-lived pollutants. *Atmos. Chem. Phys.* **15**, 10529–10566.

Tarnocai, C., Swanson, D., Kimble, J. and Broll, G. 2007. *Northern Circumpolar Soil Carbon Database, Research Branch*, Agriculture and Agri-Food Canada, Ottawa, Canada. http://wms1.agr.gc.ca/NortherCircumpolar/northercircumpolar.zip.

Thompson, R. L., Sasakawa, M., Machida, T., Aalto, T., Worthy, D. and co-authors. 2017. Methane fluxes in the high northern latitudes for 2005–2013 estimated using a Bayesian atmospheric inversion. *Atmos. Chem. Phys.* **17**, 3553–3572.

Thonat, T., Saunois, M., Bousquet, P., Pison, I., Tan, Z. and co-authors. 2017. Detectability of Arctic methane sources at six sites performing continuous atmospheric measurements. *Atmos. Chem. Phys. Discuss.* **2017**, 1–35.

Tsuruta, A., Aalto, T., Backman, L., Hakkarainen, J., van der Laan-Luijkx, I. T. and co-authors. 2017. Global methane emission estimates for 2000 six sites CarbonTracker Europe-CH4 v1.0. *Geosci. Model Dev.* **10**, 1261–1289.

Turner, A. J., Frankenberg, C., Wennberg, P. O. and Jacob, D. J. 2017. Ambiguity in the causes for decadal trends in atmospheric methane and hydroxyl. *Proc. Natl. Acad. Sci. USA* **114**, 5367–5372.

van der Laan-Luijkx, I. T., van der Velde, I. R., van der Veen, E., Tsuruta, A., Stanislawska, K. and co-authors. 2017. The CarbonTracker Data Assimilation Shell (CTDAS) v1.0: Implementation and global carbon balance 2001–2015. *Geosci. Model Dev. Discuss.* **2017**, 1–30.

Walter, K. M., Zimov, S. A., Chanton, J. P., Verbyla, D. and Chapin, F. S. 2006. Methane bubbling from Siberian thaw lakes as a positive feedback to climate warming. *Nature* **443**, 71–75.

Wania, R., Ross, I. and Prentice, I. C. 2009. Integrating peatlands and permafrost into a dynamic global vegetation model: 1. Evaluation and sensitivity of physical land surface processes. *Global Biogeochem. Cycles* **23**. doi:10.1029/2008GB003413.

Wania, R., Melton, J. R., Hodson, E. L., Poulter, B., Ringeval, B. and co-authors. 2013. Present state of global wetland extent and wetland methane modelling: Methodology of a model inter-comparison project (WETCHIMP). *Geosci. Model Dev.* **6**, 617–641.